The contribution of molecular entanglements to the rubber–elastic behaviour of electron-irradiated linear polyethylene

P. G. Klein, N. H. Ladizesky* and I. M. Ward
Department of Physics, University of Leeds, Leeds LS2 9JT, UK
(Received 21 April 1986; revised 9 October 1986; accepted 14 October 1986)

Spun polyethylene monofilaments were electron irradiated at room temperature with doses from 0.7 to 6.0 Mrad, in vacuum. Rubber elasticity experiments were performed on the as spun filaments, and filaments of draw ratio 12:1, at strain rates of 9×10^{-3} and $9 \times 10^{-2}\,s^{-1}$. The results were related to the network structure using the Flory simple statistical theory (SST), and the Mooney–Rivlin (MR) equation. The MR plots showed two straight line regions, which were assigned to the affine deformation of chemical crosslinks at low strain, and to the non-affine deformation associated with entanglement slippage at higher strain. The MR equation at low deformation gave acceptable $\bar{M}_c$ values, in close agreement with those obtained from the SST, provided the gel fraction in each case was assumed to be constant at 1.0, suggesting contributions from non-permanent network chains participating in entanglements. For the spun filaments, a linear relationship between $\bar{M}_c$ and dose was observed, and extrapolation to zero dose gave a value of $12\,000\,g\,mol^{-1}$ for the molecular weight between entanglements at 142°C. $\bar{M}_c$ showed a dependence on the strain rate, providing further evidence for non-permanent entanglement contributions. For the drawn filaments, $\bar{M}_c$ decreased in a non-linear manner with dose, and was less sensitive to strain rate. This was attributed to the deformation of the network during drawing, whereby some entanglements are pulled out, and some rendered more permanent and effective. At intermediate doses, $\bar{M}_c$ was seen to decrease up to a draw ratio of 20:1, and then increase at 30:1. This was again attributed to the effect of drawing on the structure of the entanglement network.

(Keywords: irradiated polyethylene; rubber elasticity; chain entanglements)

INTRODUCTION

The irradiation of linear polyethylene in the solid state with high energy electrons results in crosslinking, together with some main-chain scission[1]. The microstructure of polyethylene chains treated in this fashion will be complex. Above a particular irradiation dose, there will be a certain fraction of insoluble gel, consisting of chains terminated by tetrafunctional crosslinks, pendant chains, trapped entanglements, and closed loops[2]. The soluble fraction will comprise linear and branched structures of finite molecular weight which will be intimately entangled with the permanent chemical network.

Above the melt, polyethylene networks display rubberlike elasticity by virtue of the chemical crosslinks created by the irradiation. There is uncertainty as to whether the trapped and the non-permanent physical entanglements contribute to this elasticity. Treloar has argued[2] that a physical entanglement restricts the number of available chain configurations, and thus has a similar effect to a chemical crosslink. Furthermore, Treloar[3] has also suggested that the short-time elastic behaviour displayed by unvulcanized natural rubber arises from the natural entanglement network. The early experiments of Moore, Watson and Mullins[4] led to plots of 'physical' *versus* 'chemical' degrees of crosslinking, for peroxide-vulcanized rubbers, which apparently show a non-zero intercept on the physical axis, implying the presence of effective entanglements. More recent work on poly(dimethylsiloxane) networks[5] has led to the same conclusion. However, Flory[6] has critically re-interpreted this data, and concluded that trapped entanglements do not make an appreciable contribution to the modulus.

In a separate paper[7], we have investigated the structure and mechanical properties of drawn filaments produced from irradiated isotropic polyethylene. Examination of the force-extension data led us to conclude that the non-permanent physical entanglements were contributing to the stress, since the filaments displayed rubberlike elasticity below the gel point.

This paper extends this line of investigation by examining the rubber elasticity behaviour of both the spun and drawn filaments at two different extension rates. If non-permanent entanglements do contribute to the modulus in a tensile experiment, it will be a strain-rate dependent effect. At very low strain rates, there will be time for chain disentanglement and slippage to occur before the entanglements can become operative. As the strain rate is increased, a greater proportion of entanglements will contribute to the stress before slippage can occur, and this will be reflected by an increase in the modulus. The results, interpreted in terms of the apparent molecular weight between crosslinks/entanglements ($\bar{M}_c$), suggest that the entanglements do make a significant contribution, at all irradiation doses.

* Present address: Dental Materials Science Unit, The Prince Phillip Dental Hospital, University of Hong Kong, Hong Kong.

0032-3861/87/030393-06$03.00

EXPERIMENTAL

Alathon 7030 high-density polyethylene was used, $\bar{M}_n$ 28 000 g mol^{-1}, $\bar{M}_w$ 115 000 g mol^{-1}. The samples studied were monofilaments of this material, both in the as spun form, and after drawing to a nominal draw ratio of 12:1. The techniques involved in the preparation of spun monofilaments, the electron irradiation and subsequent drawing, as well as gel content determination have been described in previous papers[7,8].

Force–elongation data were obtained for the spun and drawn irradiated monofilaments, using an Instron tensile testing machine, equipped with a 500 g load cell and circulating air oven. Samples of the spun and drawn irradiated monofilaments were mounted between the clamps, which were fitted with springs to allow for sample softening above the melt. The temperature was then raised to 142°C. The initial filament lengths were about 2 cm for the spun samples, and 20 cm for the drawn samples. This allowed for the reversion to a near isotropic condition which occurs for the drawn samples above the crystalline melting temperature (~134°C). The drawn filaments required about 45 min at 142°C to reach equilibrium. Force–extension experiments were then performed at crosshead speeds of 1.25 cm min^{-1} and 12.5 cm min^{-1}, corresponding to strain rates ($\dot{\varepsilon}$) of about 9×10^{-3} s^{-1} and 9×10^{-2} s^{-1}.

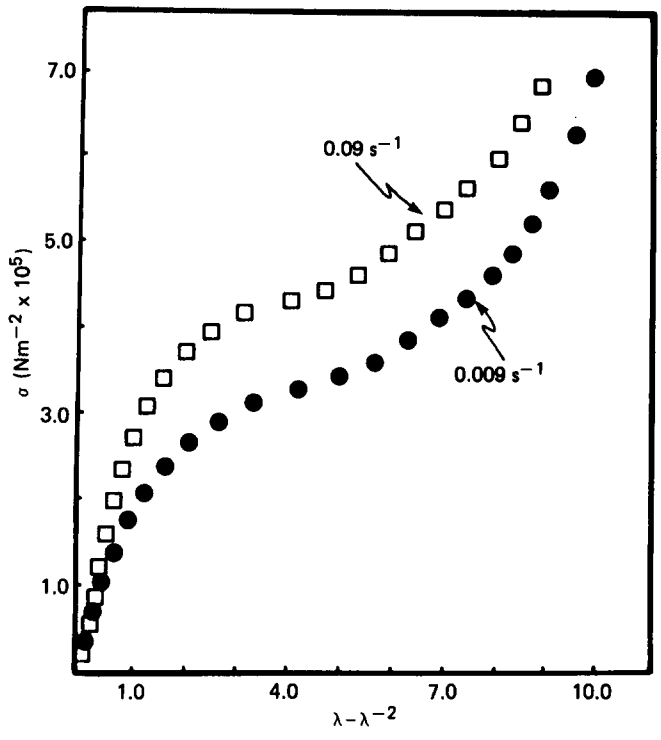

Figure 1 Stress *versus* $(\lambda-\lambda^{-2})$ for spun filament irradiated with 6.0 Mrad. The strain rate is indicated

RESULTS AND DISCUSSION

The force–extension data were interpreted in terms of the network structure via two methods: the Flory interpretation[9,10] of the simple statistical theory (SST), and by the Mooney–Rivlin[11] (MR) approach.

Simple statistical theory

The network chain density, N, is related to the shear modulus, G, via equation (1).

$$G=NkT \tag{1}$$

where k is Boltzmann's constant and T the absolute temperature. In a tensile force–extension experiment, G is approximated to $\sigma/(\lambda-\lambda^{-2})$, where σ is the force per unit unstrained area, and λ the extension ratio. In terms of $\bar{M}_c$, the number-average molecular weight between crosslinks, we have[10]:

$$\sigma/(\lambda-\lambda^{-2})=(\rho RTv_2^{2/3}/\bar{M}_c)(1-2\bar{M}_c/\bar{M}_n) \tag{2}$$

where ρ is the density, R the gas constant and v_2 the volume fraction of gel. The term in parentheses on the rhs of the equation is introduced to compensate for the elastically inactive pendant chains. The initial slope of the σ *versus* $(\lambda-\lambda^{-2})$ plot is then equated to the rhs of equation (2). A typical σ *versus* $(\lambda-\lambda^{-2})$ plot is shown in *Figure 1*.

Mooney–Rivlin theory

The MR equation[11] is an attempt to model the departure from the SST, as depicted by *Figure 1*, by introducing two empirical constants, C_1 and C_2:

$$\sigma/2(\lambda-\lambda^{-2})=C_1+C_2\lambda^{-1} \tag{3}$$

The plot of $\sigma/2(\lambda-\lambda^{-2})$ *versus* λ^{-1} should, then, be linear, of slope C_2 and intercept C_1. These parameters are then related to the network structure via the following equations[12–14]:

$$2C_1+2C_2=(\rho RTv_2^{2/3}/\bar{M}_c)(1-2\bar{M}_c/\bar{M}_n) \tag{4}$$

$$2C_1=(A_\phi\rho RTv_2^{2/3}/\bar{M}_c)(1-2\bar{M}_c/\bar{M}_n) \tag{5}$$

It can be shown that, as λ^{-1} approaches 1, $2C_1+2C_2\simeq G$. Therefore, equation (4) is applicable to low deformation, which is expected to be in the affine region. As λ^{-1} approaches zero, $G\simeq 2C_1$, in which case equation (5) is relevant to high, non-affine, deformation. Consequently, the parameter A_ϕ needs to be introduced, equal to $1-2/\phi$, where ϕ is the network functionality[12–15]. For radiation-crosslinked polyethylene, $\phi=4$, thus $A_\phi=0.5$. *Figure 2* shows how v_2 varies with irradiation dose. Up to 2.4 Mrad, there is very little (~1%) permanent network formation. Above this dose (the gel point), the gel fraction rises sharply with irradiation dose, up to 54% at 6.0 Mrad.

Figure 3 shows MR plots for the spun filaments irradiated with 6.0, 3.5 and 0.7 Mrad, at the low $\dot{\varepsilon}$. It appears that there are two separate regions of linearity; that is, C_1 and C_2 are not independent of λ, as predicted by the MR theory. At a dose of 6.0 Mrad, the slope of the line at low λ is lower than at high λ, whereas at 3.5 Mrad and below the situation is reversed. This phenomenon was previously observed[7] for the drawn samples, at low $\dot{\varepsilon}$, and has now been confirmed for both drawn and spun samples, at high and low $\dot{\varepsilon}$, although occasionally, at 6.0 Mrad, a change in slope was not observed. If a change in slope did occur for a 6.0 Mrad sample, it was never as sharp as for samples of lower dose. As before[7], we attribute the change in slope as arising out of a change from affine to non-affine deformation. For the samples irradiated with 6.0 Mrad, the reduced stress increased

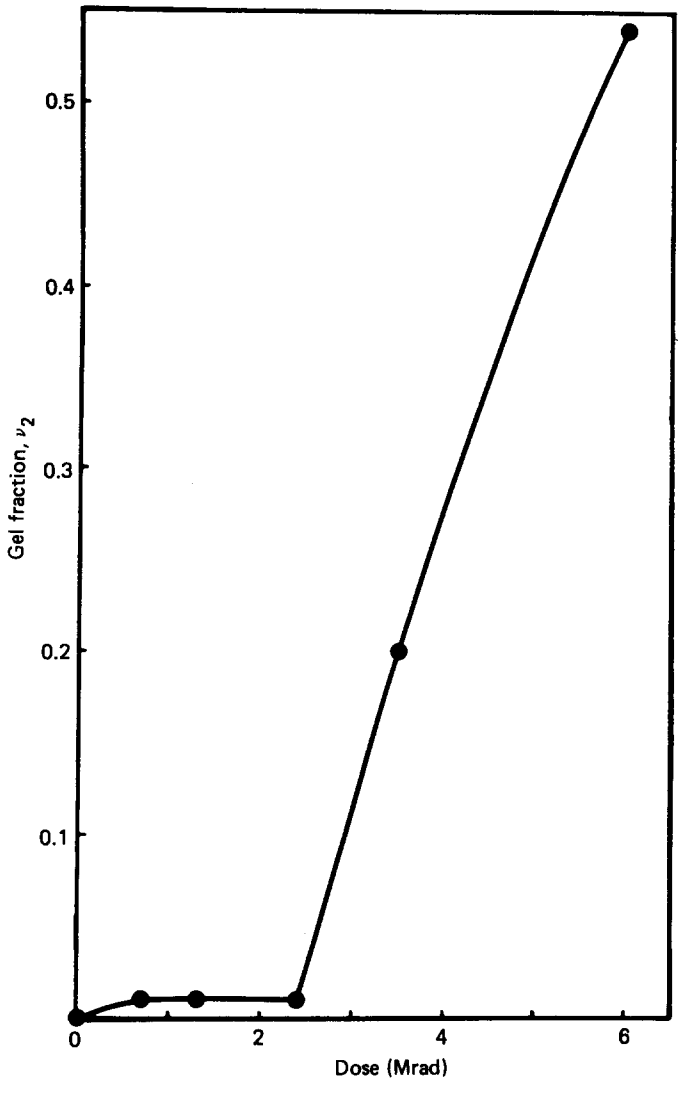

Figure 2 Gel fraction *versus* irradiation dose

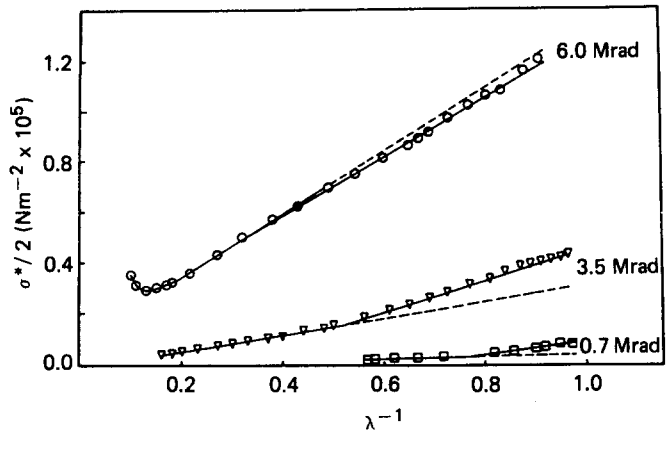

Figure 3 Mooney–Rivlin plots for spun monofilaments, at low strain rate. Irradiation doses are indicated. $\sigma^* = \sigma/(\lambda - \lambda^{-2})$

sharply at high extensions, a phenomenon observed frequently, which is attributed to the finite extensibility of the network.

In general, then, for each MR plot, two values of C_1 and C_2 were obtained, from the linear regions of the graph at high and low λ ($C^H_{1,2}$ and $C^L_{1,2}$ respectively). Consequently, equations (4) and (5) must be modified to the following expressions:

$$2C^L_1 + 2C^L_2 = (\rho RT v_2^{2/3}/\bar{M}_c)(1 - 2\bar{M}_c/\bar{M}_n) \quad (4a)$$

$$2C^H_1 = (\rho RT v_2^{2/3}/2\bar{M}_c)(1 - 2\bar{M}_c/\bar{M}_n) \quad (5a)$$

The parameter v_2 as evidence for entanglement contributions

Table 1 shows typical results obtained for the spun samples, at low $\dot{\varepsilon}$, giving $\bar{M}_c$ calculated from the SST (equation (2)) and MR theory (equations (4a) and (5a)), using the experimentally determined values of v_2, and also by assuming a v_2 value of 1.0 for all samples. Among the conclusions that may be drawn from these results are the following:

(a) The MR equation at low λ (equation (4a)), applying the experimentally determined value of v_2, results in no sensible trend between $\bar{M}_c$ and irradiation dose (column (i) in *Table 1*). The $\bar{M}_c$ values at relatively high v_2 (at 6.0 and 3.5 Mrad) are reasonable, at $\sim$5–6000 g mol^{-1}, but at a dose of 2.4 Mrad, the $\bar{M}_c$ apparently drops to $\sim$2000 g mol^{-1}. This cannot be correct, since it implies that the crosslink density is increased for a lower irradiation dose. Similarly, the $\bar{M}_c$ calculated for doses of 1.3 and 0.7 Mrad show a crosslink density equal to or greater than that obtained at a dose of 6.0 Mrad, despite a v_2 of only 1%.

(b) The $\bar{M}_c$ values shown in column (iii), obtained using the MR equation for high λ (equation (5a)), are clearly meaningless since some values are negative.

(c) Using the high λ MR equation (5a), but ignoring the $v_2^{2/3}$ parameter (i.e. assuming a gel fraction of 1.0), we obtain more satisfactory results (column (iv)). From 6.0 to 2.4 Mrad, the logical trend is observed, in that $\bar{M}_c$ increases as the irradiation dose decreases. However, below the gel point (2.4 Mrad), $\bar{M}_c$ drops, which is inconsistent with the expected effect of lower dose.

(d) The $\bar{M}_c$ calculated from the SST (equation (2)) and assuming v_2 equal to 1.0 show a logical trend between $\bar{M}_c$ and irradiation dose, for all doses applied. Furthermore, these values are in very good agreement with those obtained using the MR equation at low λ, also assuming v_2 equal to 1.0. These results are shown in columns (v) and (ii), respectively. We consider these two methods to provide the most reliable values for $\bar{M}_c$.

From the above discussion, it would appear that the term $v_2^{2/3}$ may be applicable only for samples where v_2 is

Table 1 $\bar{M}_c$ values (g mol^{-1})[a] obtained from SST and MR equations

Dose (Mrad)	$v_2^{2/3}$	$\bar{M}_c$ (MR) low λ (i)	(ii)	$\bar{M}_c$ (MR) high λ (iii)	(iv)	$\bar{M}_c$ (SST) (v)
6.0	0.66	5310	6740	11340	12130	6420
3.5	0.34	6530	10080	15480	14470	10330
2.4	0.05	2140	10970	−2460	21020	11250
1.3	0.05	3560	12210	−8910	16070	12410
0.7	0.05	5630	13030	−16570	14800	13100

[a] ± 180 g mol^{-1}
(i) Equation (4a), using experimentally determined values of v_2
(ii) Equation (4a), assuming $v_2 = 1.0$ for all samples
(iii) Equation (5a), using experimentally determined values of v_2
(iv) Equation (5a), assuming $v_2 = 1.0$ for all samples
(v) Equation (2), assuming $v_2 = 1.0$ for all samples

high, that is, where the extent of permanent network formation is sufficient to provide chemical continuity throughout the sample. At a dose of 2.4 Mrad and below, the gel content is only 1 %, such that $v_2^{2/3}$ is equal to 0.05. This causes a drastic reduction in the magnitude of the term on the rhs of equations (2), (4a) and (5a), which is not compensated by a comparable fall in the magnitude of the constants C_1 and C_2, or by a fall in the modulus, as measured by the slope of the $\sigma/\lambda - \lambda^{-2}$ plot in the SST. In other words, the modulus, as measured by the various terms in equations (2) and (4a), is much higher than that of the chemical network alone. We consider that this total modulus in each case is a combination of the moduli of the chemical network, and the non-permanent network of physical entanglements.

It has been observed[7] that a dose of 0.3 Mrad is sufficient to support the shrinkage of the drawn filaments, and a dose of 0.7 Mrad is sufficient to give rise to a detectable stress on extension. This implies that above a certain amount of irradiation, the crosslink junctions stabilize the natural molecular network, and every chain in the system is potentially elastically operative, and can contribute to the stress in a tensile experiment by means of participation in physical entanglements. Therefore, all the chains in the system should be included within the present definition of a gel, which, with regard to equations (2) and (4a), means that v_2 is equal to 1.0 for all samples. The satisfactory trend between $\bar{M}_c$ and dose shown in columns (ii) and (v) of *Table 1* provides, therefore, evidence for the manifestation of physical inter-chain entanglements.

Entanglements and the form of the Mooney–Rivlin plot

The observation of the MR plot exhibiting two straight line regions can also be interpreted within the context of entanglement contributions. Affine (low λ) deformation occurs when the microscopic deformation of network junctions mirrors the macroscopic deformation of the sample. The slippage of an entanglement, which will occur at higher λ, is a localized process; therefore the deformation accompanying the occurrence of many of these events throughout the sample must be non-affine. We therefore assign the change in slope to the onset of entanglement slippage. At high irradiation doses, the effect of chemical crosslinks is dominant, and entanglement slippage will occur only at high extension. For low doses, the amount of chemical crosslinking is very low, and entanglement slippage will occur sooner. Thus we would expect λ_T, (the extension ratio at which the transition occurs), to increase with dose. *Figure 4* shows this plot for both spun and drawn samples at both strain rates. Although there is considerable scatter in the results, it is clear that λ_T does indeed increase with dose. The straight line has been located by a linear least squares fit to all the data points, which gives an intercept on the λ_T axis of almost exactly 1.0. This provides support for the interpretation of the change in slope, since it confirms that the deformation of a hypothetical unirradiated filament would be non-affine at all strains.

The density of the entanglement network

Figures 5 and *6* show the plots of $\bar{M}_c$ *versus* dose, calculated from equation (4a) ($v_2 = 1.0$) for both the spun and drawn samples, at the two different $\dot{\varepsilon}$s. In *Table 1*, the

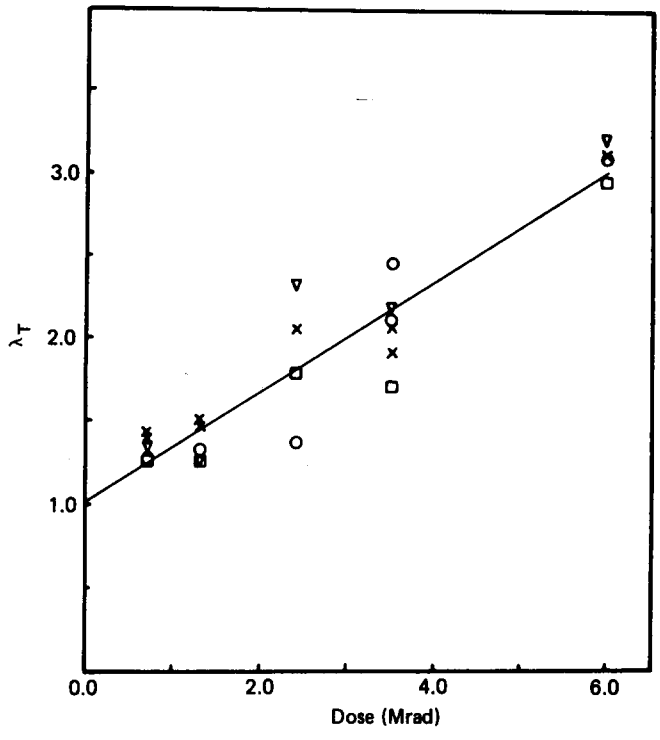

Figure 4 Extension ratio at which change in slope of Mooney–Rivlin plot occurs (λ_T), *versus* irradiation dose, for spun and drawn samples at both strain rates. (○) spun, low $\dot{\varepsilon}$; (▽) spun, high $\dot{\varepsilon}$; (×) drawn, low $\dot{\varepsilon}$; (□) drawn, high $\dot{\varepsilon}$

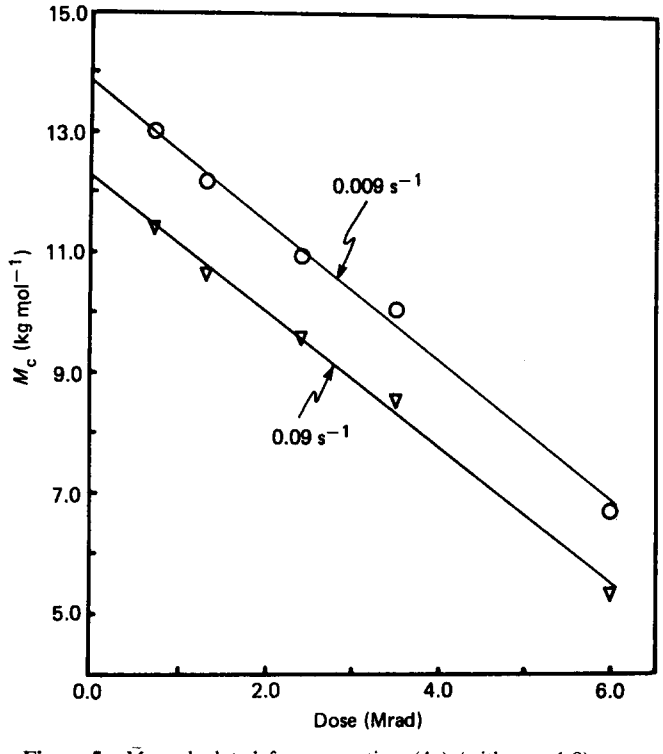

Figure 5 $\bar{M}_c$, calculated from equation (4a) (with $v_2 = 1.0$), *versus* irradiation dose, for spun filaments at the strain rates indicated

close agreement between the SST and MR methods was demonstrated for the spun samples at low $\dot{\varepsilon}$. This is also true for high $\dot{\varepsilon}$ and for the drawn samples at both $\dot{\varepsilon}$s. In the Figures, only the MR results are presented, for clarity.

For the spun samples (*Figure 5*), we can observe a linear relationship between $\bar{M}_c$ and dose, which is not reflected by the v_2 *versus* dose plot (*Figure 2*). This

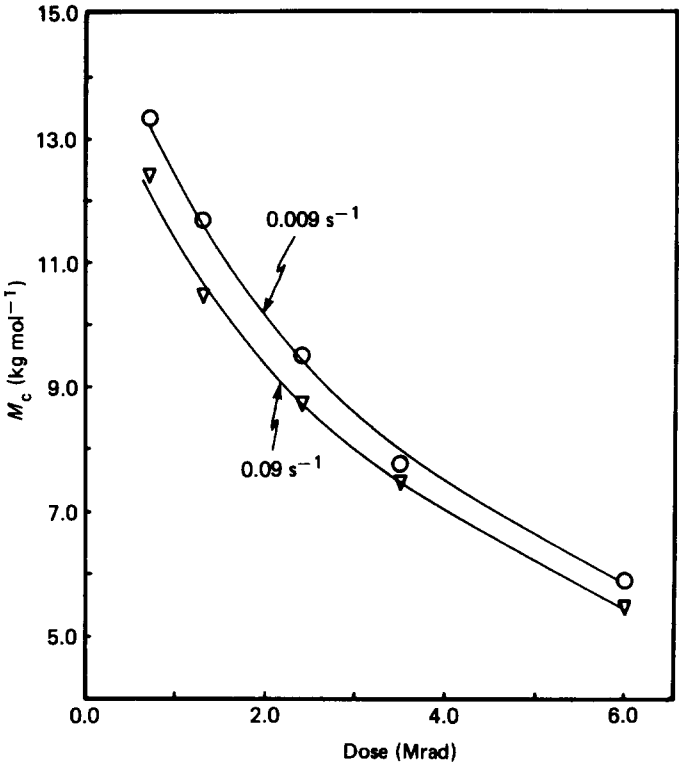

Figure 6 $\bar{M}_c$, calculated from equation (4a) (with $v_2 = 1.0$), *versus* irradiation dose, for filaments of original draw ratio 12:1, at the strain rates indicated

provides further support for the dominant role of entanglements, since it suggests that $\bar{M}_c$ depends upon the number of branch points created by the irradiation, which provide entanglement stabilization, and not the extent of chemical continuity. The linear relationship allows extrapolation back to zero dose, to arrive at an intercept value of $\sim 12\,000$ g mol^{-1}, at the higher $\dot{\varepsilon}$. This intercept represents the molecular weight between physical entanglements in the untreated polymer, at the test temperature of 142°C. We believe the extrapolation at higher $\dot{\varepsilon}$ to be the better approximation, since a greater proportion of entanglements will be taken into consideration. A recent paper by Charlesby and Jaroszkiewicz[16] considered natural entanglement formation in polystyrene. For a monodisperse polystyrene of 59 000 g mol^{-1}, various equations were derived for the temperature dependence of the entanglement concentration. These equations can be used to predict a molecular weight between entanglements of between 9400 and 12 100 g mol^{-1} at 142°C. This agrees very well with our value of $\sim 12\,000$ g mol^{-1} obtained for polyethylene, considering the difference in molecular weight, dispersity and chemical constitution.

The effect of strain rate

At low doses, the primary effect of irradiation is to stabilize the natural entanglement network, by forming a small (1%) amount of permanent chemical network, together with structures of finite molecular weight with varying degrees of branching. As the dose is increased, more highly branched polymer is created, which is more firmly entrenched within the permanent network. The gel fraction may still be very low, but the entanglements can provide a physical opposition to deformation, resulting in a measurable stress. However, at some extension, the entanglements can still slip because they are not chemically attached to the permanent network. The entanglement slippage will be a rate-dependent effect, and, therefore, the apparent $\bar{M}_c$ should also show a $\dot{\varepsilon}$ dependence, as discussed in the introduction. In the present work, we have arbitrarily chosen two values of $\dot{\varepsilon}$ an order of magnitude apart. As can be seen in *Figure 5*, $\dot{\varepsilon}$ has a significant effect on the $\bar{M}_c$ of the spun samples, suggesting that the non-permanent entanglements are contributing, at all irradiation doses.

The effect of varying $\dot{\varepsilon}$ on the $\bar{M}_c$ of the drawn filaments is much less (*Figure 6*). A further difference between spun and drawn filaments is seen in the relationship between $\bar{M}_c$ and dose. For the drawn filaments, there is an exponential type behaviour, whereas for the spun filaments the relationship is linear. We believe that the process of drawing tends to condition the samples in two ways. First, at low doses, where there is not much opposition to the slip process, some entanglements in the amorphous regions can be pulled out during the recrystallization involved in drawing. This would account for the $\bar{M}_c$ at very low doses being higher for the drawn filaments. However, it should be noted that drawing never completely eliminates the entanglement network; it has been shown from tensile creep[17,18] and shrinkage force[19] experiments that for drawn, unirradiated filaments, there is still an effective molecular network present even at draw ratios of 30 and above. Secondly, at higher doses, the molecular branching is more extensive and fewer chain entanglements can be removed in drawing. Those that remain in the system after drawing become more permanent and more entrenched, accounting for the relative insensitivity to $\dot{\varepsilon}$. At a dose of 2.4 Mrad and above, the $\bar{M}_c$ for the drawn samples is generally less than for the spun filaments, suggesting that drawing has, in some way, brought into operation those entanglements which previously were ineffective.

The effect of draw ratio

Further information on the influence of drawing an entanglement structure may be obtained from *Figure 7*, which shows plots of $\bar{M}_c$ *versus* draw ratio, for filaments irradiated with various doses. There is a limitation on the information that can be gained from these experiments, since the filament irradiated with 6.0 Mrad cannot be drawn to more than 12:1, and the 3.5 Mrad filament no more than 20:1[8]. However, the results at 2.4 Mrad are particularly informative. This shows $\bar{M}_c$ decreasing with draw ratio up to 20:1, and then increasing at 30:1. This suggests that, up to draw ratio 20, drawing makes the entanglements more effective and permanent, but above this draw ratio, the forces imposed on the network are such that entanglement slippage occurs, leading to a looser overall network. The results for the filaments irradiated to 3.5 Mrad indicate a similar trend, whereas those for the 6.0 Mrad sample show $\bar{M}_c$ to be largely independent of draw ratio. This is not surprising, since at this dose, the effect of non-permanent entanglements will be largely superseded by the effect of the continuous permanent network.

CONCLUSIONS

The contention that molecular entanglements contribute to rubber elasticity behaviour has been supported by

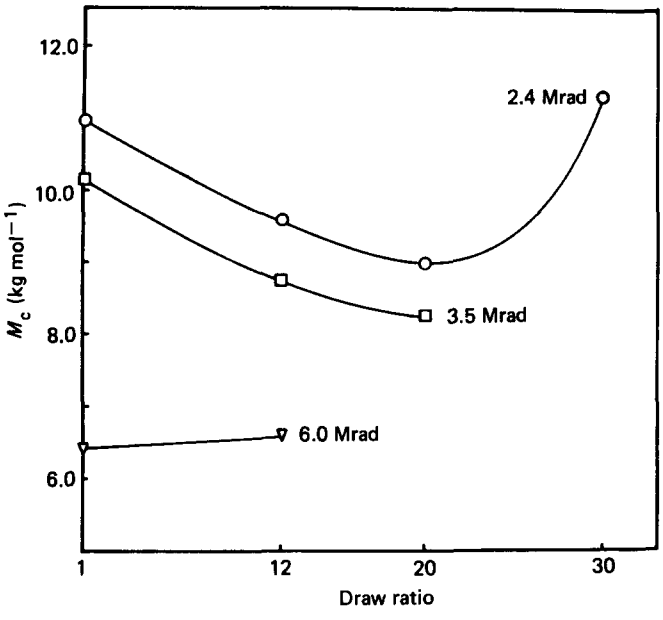

Figure 7 $\bar{M}_c$ *versus* draw ratio for filaments irradiated with the doses indicated, at low $\dot{\varepsilon}$. The $\bar{M}_c$ values are averages of results obtained from SST and MR methods

experiments on electron-irradiated polyethylene filaments. Indications of the effective presence of non-permanent entanglements, that is, those chains that can be removed by solvent extraction, comes from the following observations: (i) The Mooney–Rivlin equation leads to satisfactory M_c values only at low deformation, and assuming a constant gel fraction of 1.0. (ii) $\bar{M}_c$ for both the spun and drawn filaments decreases steadily with dose, with no sharp discontinuity at the gel point, and (iii) $\bar{M}_c$ shows a dependence on both the strain rate and on the original draw ratio of the filaments.

The observation that the MR plot is not linear over the entire λ range can be interpreted in terms of a change from affine to non-affine deformation, and satisfactory results may be obtained by considering only the low λ region of the plot. However, we believe that a better description of the deviations from the SST can be obtained from the Edwards slip-link model for chain entanglements[20,21]. Preliminary calculations have been encouraging, and we are at present attempting to quantify the chain entanglement contribution using this theory.

REFERENCES

1 Charlesby, A. and Pinner, S. H. *Proc. Roy. Soc.* 1959, **A249**, 367; Ungar, G. and Keller, A. *Polymer* 1980, **21**, 1273
2 Treloar, L. R. G., 'The Physics of Rubber Elasticity', 3rd Edn., Oxford University Press, 1975, pp. 74–75
3 Treloar, L. R. G., 'Introduction to Polymer Science', Wykeham Publications, London, 1982, p. 46
4 Ref. 2, pp. 167–173
5 Kirk, K. A., Bidstrup, S. A., Merrill, E. W. and Meyers, K. O. *Macromolecules* 1982, **15**, 1123
6 Flory, P. J. and Erman, B. *J. Polym. Sci., Polym. Phys. Edn.* 1984, **22**, 49
7 Klein, P. G., Ladizesky, N. H. and Ward, I. M. *J. Polym. Sci., Polym. Phys. Edn.* 1986, **24**, 1093
8 Ladizesky, N. H., Chaoting, Y. and Ward, I. M. *J. Macromol. Sci., (Phys.)* 1986, **B25**, 185
9 Flory, P. J. *Chem. Rev.* 1944, **35**, 51
10 Flory, P. J. *Ind. Eng. Chem.* 1946, **38**, 417
11 Mooney, M. *J. Appl. Phys.* 1948, **19**, 434; Rivlin, R. S. *Phil. Trans. Roy. Soc. London Ser. A* 1948, **241**, 379
12 Llorente, M. A. and Mark, J. E. *J. Chem. Phys.* 1979, **71**, 682
13 Llorente, M. A. and Mark, J. E. *Macromolecules* 1980, **13**, 681
14 Llorente, M. A., Andrady, A. L. and Mark, J. E. *J. Polym. Sci., Polym. Phys. Edn.* 1981, **19**, 621
15 Mark, J. E. and Sullivan, J. L. *J. Chem. Phys.* 1977, **66**, 1006
16 Charlesby, A. and Jaroszkiewicz, E. M. *Eur. Polym. J.* 1985, **21**, 55
17 Wilding, M. A. and Ward, I. M. *Polymer* 1981, **22**, 870
18 Ward, I. M. and Wilding, M. A. *J. Polym. Sci., Polym. Phys. Edn.* 1984, **22**, 561
19 Capaccio, G. and Ward, I. M. *Colloid Polym. Sci.* 1982, **260**, 46
20 Ball, R. C., Doi, M., Edwards, S. F. and Warner, M. *Polymer* 1981, **22**, 1010
21 Thirion, P. and Weil, T. *Polymer* 1984, **25**, 609